JCB Report

Mice with defects in HB-EGF ectodomain shedding show severe developmental abnormalities

Satoru Yamazaki,[1] Ryo Iwamoto,[1] Kazuko Saeki,[2] Masanori Asakura,[3] Seiji Takashima,[3] Ayano Yamazaki,[1] Rina Kimura,[1] Hiroto Mizushima,[1] Hiroki Moribe,[1] Shigeki Higashiyama,[6] Masayuki Endoh,[4] Yasufumi Kaneda,[4] Satoshi Takagi,[5] Satoshi Itami,[5] Naoki Takeda,[7] Gen Yamada,[7] and Eisuke Mekada[1]

[1]Research Institute for Microbial Diseases, Osaka University, Osaka 565-0871, Japan
[2]Medical Institute of Bioregulation, Kyushu University, Fukuoka 812-8582, Japan
[3]Department of Internal Medicine and Therapeutics, [4]Division of Gene Therapy Science, and [5]Department of Dermatology, Graduate School of Medicine, Osaka University, Osaka 565-0871, Japan
[6]Department of Medical Biochemistry, Ehime University School of Medicine, Ehime 791-0295, Japan
[7]Center for Animal Resource and Development and Graduate School of Molecular and Genomic Pharmacy, Kumamoto University, Kumamoto 860-0811, Japan

Heparin-binding EGF-like growth factor (HB-EGF) is first synthesized as a membrane-anchored form (proHB-EGF), and its soluble form (sHB-EGF) is released by ectodomain shedding from proHB-EGF. To examine the significance of proHB-EGF processing in vivo, we generated mutant mice by targeted gene replacement, expressing either an uncleavable form (HB^{uc}) or a transmembrane domain–truncated form ($HB^{\Delta tm}$) of the molecule. $HB^{uc/uc}$ mice developed severe heart failure and enlarged heart valves, phenotypes similar to those in proHB-EGF null mice. On the other hand, mice carrying $HB^{\Delta tm}$ exhibited severe hyperplasia in both skin and heart. These results indicate that ectodomain shedding of proHB-EGF is essential for HB-EGF function in vivo, and that this process requires strict control.

Introduction

Heparin-binding EGF-like growth factor (HB-EGF), a member of the EGF family, binds the EGF receptor (EGFR) and ErbB4 to initiate signaling (Higashiyama et al., 1991; Elenius et al., 1997). Like other EGF family members (for review see Massague and Pandiella, 1993), HB-EGF is first synthesized as a membrane-anchored form (proHB-EGF), and then the soluble form (sHB-EGF) is released from the cell surface by ectodomain shedding (Goishi et al., 1995). sHB-EGF is a diffusible factor with potent mitogenic and chemoattractant activities for a number of cell types. ProHB-EGF forms a complex with other membrane proteins at the cell–cell contact site and transduces biological signals to neighboring cells in a nondiffusible manner (for review see Iwamoto and Mekada, 2000). Thus, in addition to being a precursor of sHB-EGF, proHB-EGF is thought to be a biologically active molecule itself. Several studies in vitro have revealed that a number of signaling molecules control the ectodomain shedding of proHB-EGF (Izumi et al., 1998; Umata et al., 2001; Takenobu et al., 2003), implying that strict control of ectodomain shedding is critical for HB-EGF function.

Recently, we demonstrated that HB-EGF is critical for proper heart development and function by the analyses of HB-EGF null mice (Iwamoto et al., 2003). However, it remains unclear which forms of HB-EGF are necessary for these process. The relative roles of either proHB-EGF or sHB-EGF and the significance of the control of ectodomain shedding in vivo have yet to be determined. To address these issues, we generated two kinds of mutant mice, by targeted gene replacement, that express either an uncleavable (HB^{uc}) or a transmembrane domain–truncated form ($HB^{\Delta tm}$) of proHB-EGF. Analysis of these mutant lines indicates that

S. Yamazaki and R. Iwamoto contributed equally to this work.

The online version of this article includes supplemental material.

Address correspondence to Eisuke Mekada, Department of Cell Biology, Research Institute for Microbial Diseases, Osaka University, Osaka 565-0871, Japan. Tel.: 81-6-6879-8286. Fax: 81-6-6879-8289. email: emekada@biken.osaka-u.ac.jp

Key words: ectodomain shedding; ErbB; cardiomyopathy; valvulogenesis; epidermal hyperplasia

Abbreviations used in this paper: EGFR, EGF receptor; HB-EGF, heparin-binding EGF-like growth factor; proHB-EGF, membrane-anchored form of HB-EGF; sHB-EGF, soluble form of HB-EGF; TPA, *O*-tetradecanoylphorbol-13-acetate; tRA, all-trans retinoic acid.

© The Rockefeller University Press, 0021-9525/2003/11/469/7 $8.00

The Journal of Cell Biology

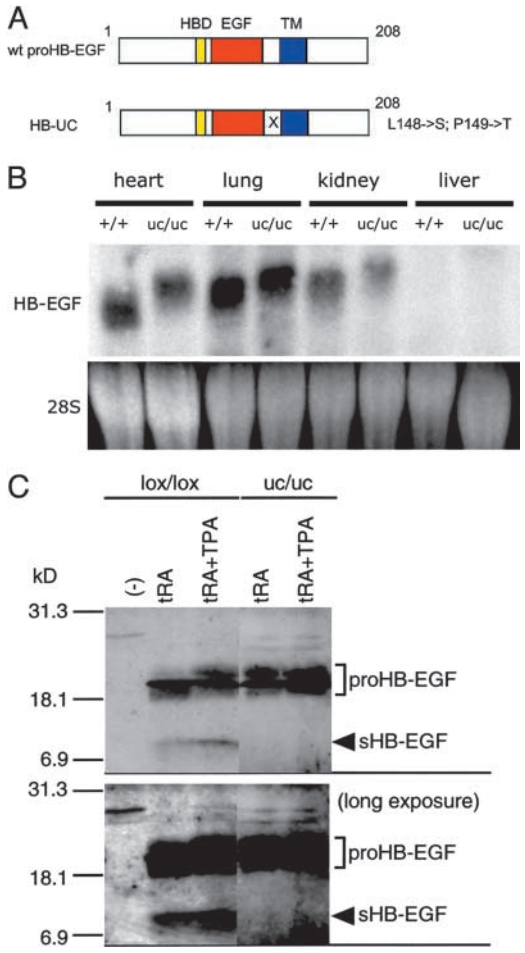

Figure 1. **Expression and uncleavability of HB-UC in HB^{uc} knock-in mice.** (A) Schematic structures of the HB-UC constructs. HBD, heparin-binding domain; EGF, EGF-like domain; TM, transmembrane domain. (B) Northern blot analysis of HB-EGF mRNA from adult WT (+/+) and HB$^{uc/uc}$ (uc/uc) mice. The size of the transcript from HB^{uc} is 100 bp larger than that from the WT gene due to neo cassette integration. (C) Uncleavable HB-UC in tRA- and TPA-treated skin. HB-EGF immunoblots of protein extracted and concentrated by heparin-Sepharose from 11-wk-old control (lox/lox) or HB$^{uc/uc}$ (uc/uc) mouse skin, treated with tRA (tRA), TPA after tRA treatment (tRA + TPA), or no treatment (−).

proHB-EGF shedding is essential in vivo and that this process must be controlled.

Results and discussion

Generation of mice expressing uncleavable proHB-EGF mutant

An uncleavable form of proHB-EGF was generated by creating double point mutations, L148S/P149T, in the juxtamembrane domain (designated HB^{uc}) (Fig. 1 A). As shown previously in cases of each single point mutation (Hirata et al., 2001), HB-UC (a product of HB^{uc}) was also resistant to ectodomain shedding in response to various shedding-inducing stimuli, while the other biological properties of HB-UC were similar to those of WT proHB-EGF (Fig. S1, A–C, and supplemental Results, available at http://www.jcb.org/cgi/content/full/jcb.200307035/DC1). To assess the biological significance of proHB-EGF ectodomain shedding, we created mutant mice expressing HB-UC instead of WT proHB-EGF by targeted replacement of the proHB-EGF gene with HB^{uc} cDNA (Fig. S2, supplemental Results, and supplemental Materials and methods, available at http://www.jcb.org/cgi/content/full/jcb.200307035/DC1). Homozygous mice (HB$^{uc/uc}$) were born at the predicted Mendelian frequency. Northern blotting of the transcripts obtained from adult mice indicated that the WT and HB^{uc} alleles were expressed equally in heart, lung, and kidney (Fig. 1 B).

We examined whether HB-UC was resistant to ectodomain shedding in mice (Fig. 1 C). We used adult mouse skin samples obtained from HB$^{uc/uc}$ mice and HB$^{lox/lox}$ mice as a control. In HB$^{lox/lox}$ mice, the proHB-EGF locus was replaced with WT proHB-EGF cDNA (Iwamoto et al., 2003), making HB$^{lox/lox}$ mice more suitable controls than WT mice. In adult mouse skin, HB-EGF protein bands were hardly detected in samples obtained from adult HB$^{uc/uc}$ and HB$^{lox/lox}$ mice. All-trans retinoic acid (tRA) is known to induce HB-EGF expression, followed by epidermal hyperplasia (Xiao et al., 1999). When tRA was applied to skin on the backs of mice, proHB-EGF protein was induced and clearly detected in samples from HB$^{lox/lox}$ and HB$^{uc/uc}$ mice by using an antibody against the proHB-EGF ectodomain. Under these conditions, the band corresponding to sHB-EGF was also detected in HB$^{lox/lox}$ mice, but not in HB$^{uc/uc}$ mice. An antibody recognizing the cytoplasmic domain of proHB-EGF did not detect this sHB-EGF band (unpublished data), confirming that this band corresponds to secreted HB-EGF. When tRA-induced skin was further treated with *O*-tetradecanoylphorbol-13-acetate (TPA), the sHB-EGF band appeared more intensely in HB$^{lox/lox}$ mice. However, the sHB-EGF band was not detected in samples from tRA + TPA–treated HB$^{uc/uc}$ mice. These results indicate that ectodomain shedding of proHB-EGF is severely impaired in HB$^{uc/uc}$ mice.

Uncleavable proHB-EGF mutation causes cardiac dysfunction and heart valve malformation

Recently, we showed that HB-EGF null mice (HB$^{del/del}$) have defects in cardiac chamber dilation and cardiac valve malformation (Iwamoto et al., 2003). Therefore, we analyzed the heart phenotype in HB$^{uc/uc}$ mice. Autopsies of HB$^{uc/uc}$ mice revealed massive enlargement of the heart. Histological analysis showed that wall thickness was reduced, accompanied by sporadic fibrosis in 12-wk-old HB$^{uc/uc}$ mice (Fig. 2, A–D). These phenotypes are highly similar to those observed in HB-EGF null mice (Iwamoto et al., 2003) and ErbB2 conditional knockout mice (Crone et al., 2002; Ozcelik et al., 2002).

Transthoracic echocardiography indicated marked dilation and poor left ventricular contraction in HB$^{uc/uc}$ mice (Fig. 2, E and F). Dilation could be detected in 4-wk-old mice, though the physical activity level and appearance was indistinguishable between WT and HB$^{uc/uc}$ mice. Mutant mice also had reduced cardiac wall movement, and ventricular fractional shortening (FS), a representative measure of systolic function, was greatly reduced.

In addition to the ventricular chamber abnormality, heart valve malformation was also observed in HB$^{uc/uc}$ mice as in HB-EGF null mice (Iwamoto et al., 2003; Jackson et al.,

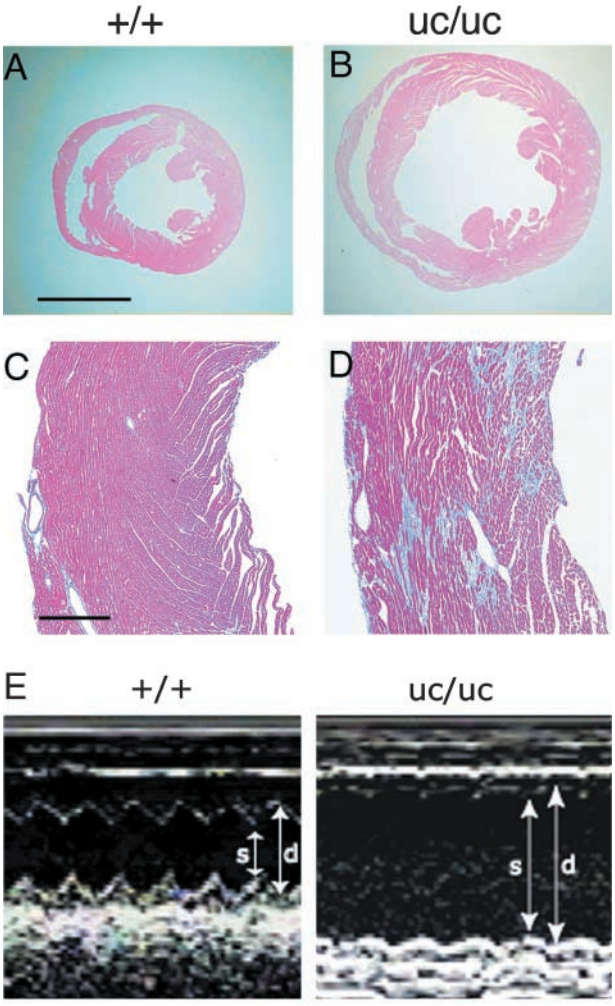

F

	+/+ (n=10)	uc/uc (n=13)	p-value
HR (/min)	630.9±79.3	644.0±60.1	n.s
sBP (mmHg)	102.3±6.4	93.3±8.1	p<0.05
dBP (mmHg)	64.4±7.8	55.4±6.4	p<0.05
LVDd (mm)	3.17±0.24	4.86±0.73	p<0.001
LVDs (mm)	2.04±0.29	3.80±0.84	p<0.001
FS (%)	35.7±4.8	22.5±7.3	p<0.001

Figure 2. **Histological and echocardiographic analysis of hearts from adult HB$^{uc/uc}$ mice.** (A and B) Hematoxylin-eosin staining of transverse sections through hearts of 12-wk-old mice at the papillary muscle level. Bar, 3 mm. (C and D) High magnification pictures. Sections were stained with Azan-Mallory. Massive fibrosis (blue stain) is present in 12-wk-old HB$^{uc/uc}$ heart throughout the vessel wall. Bar, 250 μm. (E and F) Echocardiographic analyses of hearts from WT (+/+) and HB$^{uc/uc}$ (uc/uc) mice. (E) Representative images of M-mode analyses are shown. Arrows indicate end-diastolic (d) and end-systolic (s) dimensions, respectively. (F) Physiological parameters of WT versus HB$^{uc/uc}$ hearts in 12-wk-old mice. HR, heart rate; sBP and dBP, systolic and diastolic blood pressure; LVDd and LVDs, left ventricular end diastolic and end systolic internal dimensions; FS, percent fractional shortening calculated as [(LVDd − LVDs)/LVDd] × 100. All values ± SEM.

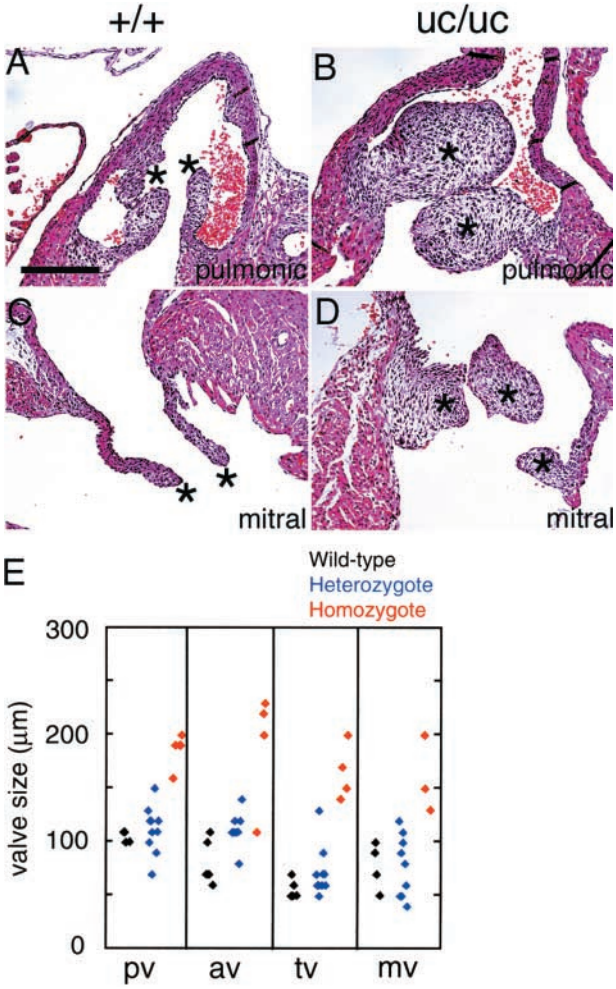

Figure 3. **Cardiac valve defects in HB$^{uc/uc}$ mice.** (A–D) Histological analysis of cardiac valves. Shown are hematoxylin-eosin–stained longitudinal sections of hearts of E17.5 embryos. Mice are WT (A and C) and HB$^{uc/uc}$ (B and D). Pulmonic (A and B) and mitral valves (C and D) are indicated by asterisks. Aortic and tricuspid valves were also enlarged (not depicted). Bar, 150 μm. (E) Measurement of cardiac valve size. The largest diameters of each valve in serial sections of E17.5 embryos of WT (black dots, $n = 5$), HB$^{uc/+}$ (blue dots, $n = 9$), and HB$^{uc/uc}$ (red dots, $n = 4$) hearts were measured. pv, pulmonic valve; av, aortic valve; tv, tricuspid valve; mv, mitral valve.

2003) and EGFR knockout mice (Chen et al., 2000). Histological analysis of E17.5 embryonic HB$^{uc/uc}$ hearts showed enlarged semilunar (aortic and pulmonic) and atrioventricular (mitral and tricuspid) valves (Fig. 3, A–D). Scoring of cardiac valve size in E17.5 hearts revealed enlarged semilunar and atrioventricular valves in HB$^{uc/uc}$ mice (Fig. 3 E). No overt abnormality was observed in HB$^{lox/lox}$ heart chambers or valves (Iwamoto et al., 2003), indicating that heart abnormalities in HB$^{uc/uc}$ mice were not due to a nonspecific effect of cDNA knock-in.

The similar heart defects displayed in HB$^{del/del}$ and HB$^{uc/uc}$ mice indicate that the process of ectodomain shedding is essential for HB-EGF function in normal cardiac valve development and cardiomyocyte function, and that soluble HB-EGF is required for these processes. We also examined whether proHB-EGF has any in vivo physiological role aside from acting as the sHB-EGF precursor. Interestingly, HB$^{del/del}$ mice

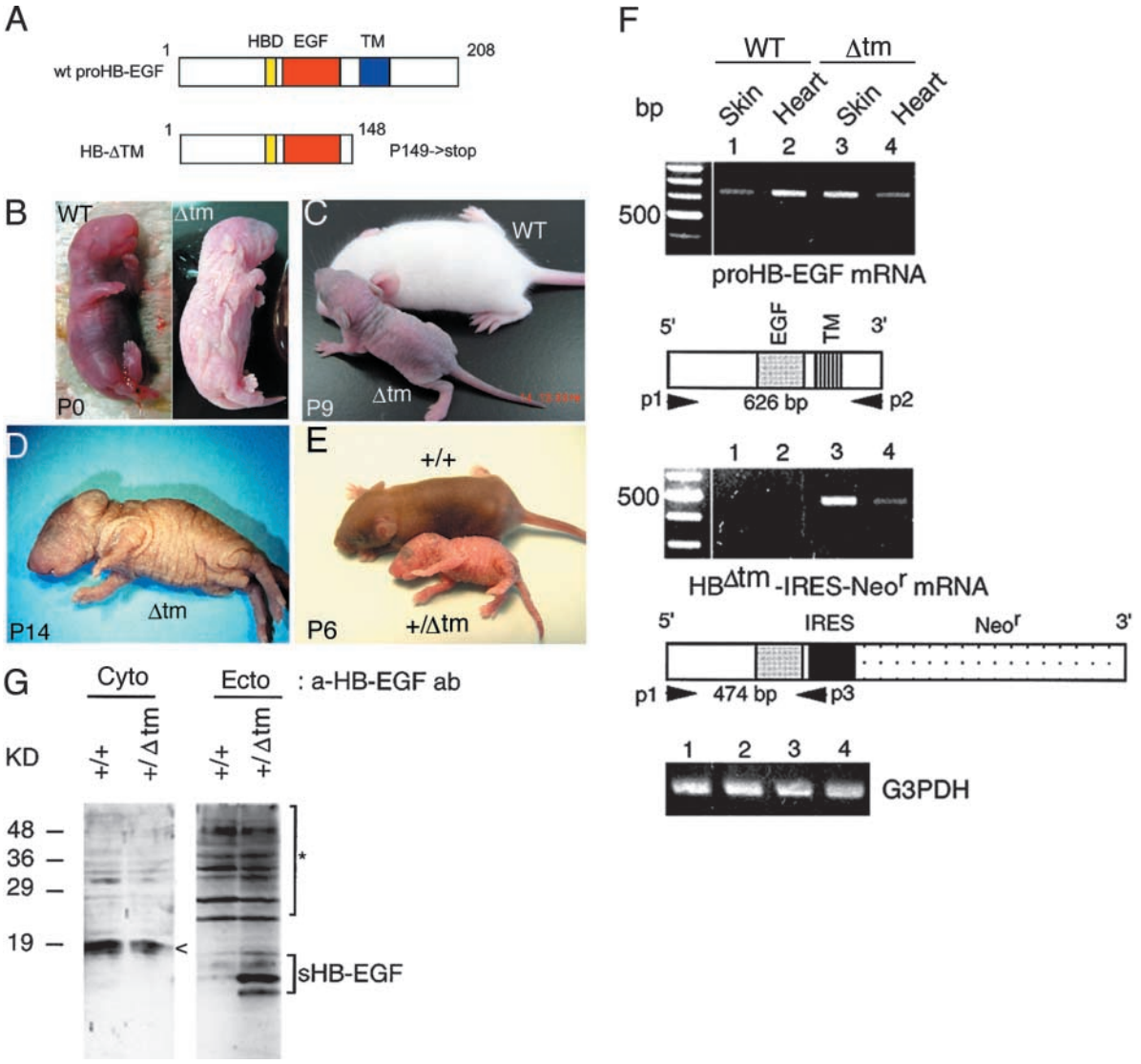

Figure 4. **HB$^{\Delta tm}$ knock-in mice.** (A) Schematic structures of the HB-ΔTM construct. (B–D) Phenotype of HB$^{\Delta tm}$ chimeric mice. P0 (B) and P9 (C) wild-type (WT) and HB$^{\Delta tm}$ chimeric (Δtm) mice and P14 HB$^{\Delta tm}$ chimeric mice (D) are shown. (E) Phenotype of P6 HB$^{\Delta tm}$ heterozygous mice (+/Δtm) and wild-type littermates (+/+). (F and G) Expression of HB$^{\Delta tm}$ in the targeted mice. (F) Transcription of the HB$^{\Delta tm}$ allele was assessed by RT-PCR analysis of tissues (skin and heart) from P14 wild-type (WT) and chimeric (Δtm) mice. Primer sets detecting the wild-type (p1 and p2) or HB$^{\Delta tm}$ allele (p1 and p3) transcripts are indicated below each gel. EGF, EGF-like domain; TM, transmembrane domain. RT-PCR with primer sets for the detection of GAPDH transcripts is shown in the lower panel as a loading control. (G) Detection of sHB-EGF in the skin. Immunoblots of proteins (150 μg/lane) extracted from P1 WT (+/+) or heterozygous (+/Δtm) mouse skin were performed using anti–proHB-EGF antibodies that recognize either intracellular (Cyto) or extracellular regions (Ecto) of HB-EGF. The extracellular-specific antibody detects sHB-EGF more efficiently than proHB-EGF. Four major bands corresponding to sHB-EGF, resulting from multiple processing and glycosylation sites in the HB-EGF NH_2-terminal region, were detected in HB$^{\Delta tm}$ heterozygous mice. Arrowheads indicate the bands corresponding to proHB-EGF. The asterisk indicates nonspecific bands.

displayed a shorter life span than HB$^{uc/uc}$ mice. Half of HB$^{uc/uc}$ mice survive over 18 wk, while >60% of HB$^{del/del}$ mice died in the first postnatal week. These differences between HB$^{del/del}$ and HB$^{uc/uc}$ mice suggest that proHB-EGF may function in unidentified developmental processes. Further comparison of the phenotypes between HB$^{del/del}$ and HB$^{uc/uc}$ mice may help us answer this question.

Generation of mice expressing soluble proHB-EGF mutant

Although studies of HB$^{uc/uc}$ mice indicated that ectodomain shedding of proHB-EGF and release of sHB-EGF is necessary for proper HB-EGF function in vivo, the physiological importance of the control of proHB-EGF ectodomain shedding remained unclear. To address this issue, we prepared another mouse mutant that only expresses sHB-EGF. The transmembrane domain–truncated mutant (HB$^{\Delta tm}$) was generated by insertion of a stop codon between Leu^{148} and Pro^{149} (Fig. 4 A), the major site for proHB-EGF processing (Higashiyama et al., 1992). Mitogenic activity was similar between HB-ΔTM (product of HB$^{\Delta tm}$) and WT sHB-EGF derived from proHB-EGF shedding, but HB-ΔTM is secreted at much higher levels than WT sHB-EGF (Fig. S1, D–G, and supplemental Results). The targeting construct

The Journal of Cell Biology

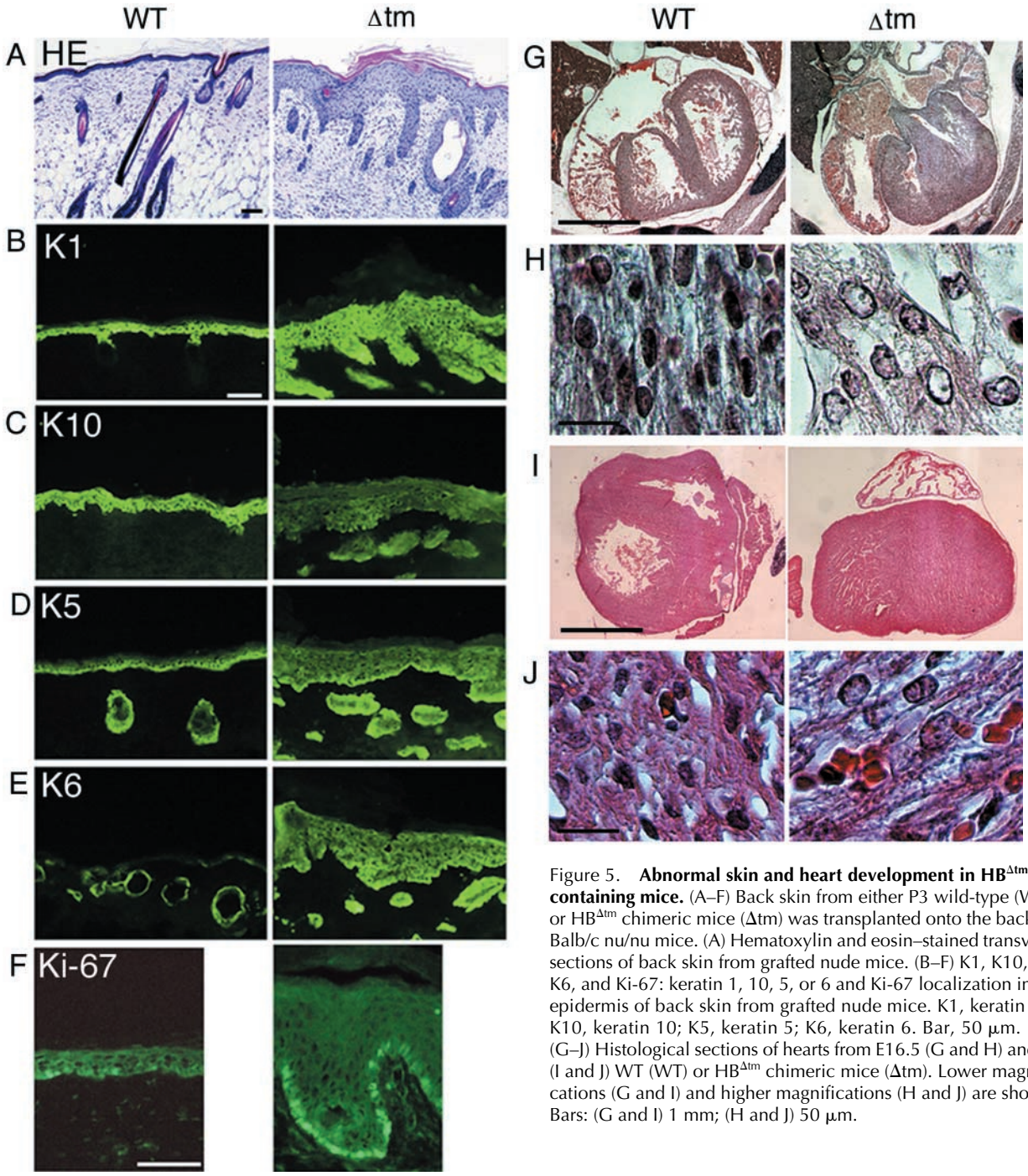

Figure 5. **Abnormal skin and heart development in HB$^{\Delta tm}$-containing mice.** (A–F) Back skin from either P3 wild-type (WT) or HB$^{\Delta tm}$ chimeric mice (Δtm) was transplanted onto the backs of Balb/c nu/nu mice. (A) Hematoxylin and eosin–stained transverse sections of back skin from grafted nude mice. (B–F) K1, K10, K5, K6, and Ki-67: keratin 1, 10, 5, or 6 and Ki-67 localization in the epidermis of back skin from grafted nude mice. K1, keratin 1; K10, keratin 10; K5, keratin 5; K6, keratin 6. Bar, 50 μm. (G–J) Histological sections of hearts from E16.5 (G and H) and P0 (I and J) WT (WT) or HB$^{\Delta tm}$ chimeric mice (Δtm). Lower magnifications (G and I) and higher magnifications (H and J) are shown. Bars: (G and I) 1 mm; (H and J) 50 μm.

for HB$^{\Delta tm}$ is similar to that for HB^{uc}. One allele of the proHB-EGF gene in ES cells was replaced with HB$^{\Delta tm}$ through homologous recombination (Fig. S2, supplemental Results, and supplemental Materials and methods). Chimeric mice carrying HB$^{\Delta tm}$ were generated from these ES clones. Most chimeric founders exhibited abnormally small bodies and thickened skin (Fig. 4, B–D). The majority of these mice died before or during the neonatal stage (unpublished data). A few mice, however, survived and were fertile. Most of the resulting F1 heterozygotes carrying the HB$^{\Delta tm}$ allele also died before or during the neonatal stage (unpublished data), displaying a more severe phenotype than that seen in chimeric mice (Fig. 4 E).

We confirmed the expression of the HB$^{\Delta tm}$ cDNA in chimeric mice by RT-PCR of skin and heart specimens (Fig. 4 F). Transcripts derived from the WT proHB-EGF allele were detected in both WT and chimeric tissues, while those derived from the HB$^{\Delta tm}$ allele were only identified in chimeric mice. Expression of HB$^{\Delta tm}$ was also confirmed at the protein level using anti–HB-EGF antibody, specific for the extracellular domain of proHB-EGF. In heterozygote skin, significant quantities of soluble HB-EGF were detected, whereas sHB-EGF protein was only barely detectable in WT skin (Fig. 4 G). The quantities of proHB-EGF with a molecular mass of ~19 kD, detected by an anti–HB-EGF antibody specific for the cytoplasmic domain, displayed a con-

comitant decrease in heterozygote skin relative to the levels seen in wild-type skin (Fig. 4 G).

Dysregulated release of HB-EGF induces developmental abnormalities with hyperplasia

The most obvious phenotype of $HB^{\Delta tm}$-carrying mice, distinguishing them from WT mice, was the presence of abnormal elephant-like skin (Figs. 4, B–E). $HB^{\Delta tm}$ mice have short lives; thus to further study the epidermal hyperplasia, back skin was transplanted from P3 WT or $HB^{\Delta tm}$ chimeric mice onto the backs of Balb/c nu/nu mice for 2 wk. This transplantation method also allowed for the specific examination of the effects of $HB^{\Delta tm}$ in the skin in an animal with otherwise normal expression and processing of HB-EGF. Histological examination revealed severe epidermal hyperplasia, accompanied by the presence of large, disorganized, hair follicle–like structures (Fig. 5 A). Immunohistochemistry of epidermal marker proteins revealed perturbed differentiation and proliferation of keratinocytes (Fig. 5, B–F). Keratin 5, normally expressed by both mitotically active, basal layer keratinocytes and hair follicles, was detected in the suprabasal epidermis of chimeric mice (Fig. 5 D). Keratin 1, normally expressed by differentiating keratinocytes in the suprabasal epidermis, but not by the cells of the hair follicle (Heid et al., 1988), was expressed in the hair follicle–like structures of chimeric mice (Fig. 5 B). Additionally, keratin 10, a differentiating keratinocyte marker, was down-regulated in chimeric mice (Fig. 5 C). Keratin 6, expressed predominantly in hair follicle cells, and at lower levels in the suprabasal epidermis, was detected throughout the epidermis of chimeric mice (Fig. 5 E), consistent with the induction of keratin 6 expression by epidermal hyperproliferation (Werner et al., 1993). The expression of Ki-67, a nuclear mitotic marker, was also increased in the basal layer of chimeric skin compared with levels seen in WT (Fig. 5 F), indicating that $HB^{\Delta tm}$ expression accelerates basal layer keratinocyte proliferation. No overt abnormality was observed in the skin area surrounding the transplanted skin, suggesting that the abnormality in the transplanted skin is due to the action of HB-ΔTM in a manner of autocrine or paracrine in limited distance, rather than paracrine in long distance.

Morphological abnormalities were also found in the heart of $HB^{\Delta tm}$ mice. Histological specimens showed ventricular hypertrophy in hearts from $HB^{\Delta tm}$ E16.5 embryos (Fig. 5 G) and P0 mice (Fig. 5 I). HB-EGF is expressed in cardiomyocytes (Iwamoto et al., 2003), consistent with the present results. The cardiac muscle fibers in chimeric mice were loose, with enlarged nuclei (Fig. 5, H and J). These results suggest that expression of $HB^{\Delta tm}$ reduces cardiomyocyte differentiation or terminates proliferation. These cardiac developmental abnormalities may be the primary cause of early death in $HB^{\Delta tm}$ mice.

The phenotype observed in $HB^{\Delta tm}$ mice is likely due to dysregulated secretion of sHB-EGF. In normal conditions, a portion of proHB-EGF molecules are converted to sHB-EGF, but the majority of proHB-EGF molecules on the cell surface seems to be internalized without shedding (Goishi et al., 1995). In the case of $HB^{\Delta tm}$, most synthesized molecules would be secreted without shedding, resulting in oversecretion of sHB-EGF even though the native HB-EGF promoter regulates gene expression. Therefore, dysregulated secretion of sHB-EGF would result in severe developmental abnormalities. The present study thus confirms the notion that ectodomain shedding of proHB-EGF must be strictly controlled in vivo.

One question regarding the truncated $HB^{\Delta tm}$ mutant concerns whether the observed hyperplasia might be due to an intracrine rather than a paracrine mechanism. A transmembrane domain–truncated EGF mutant was reported to activate EGFR in an intracrine manner, as a result of interaction with EGFR within cytoplasmic vesicles, before the molecules reached the cell surface (Wiley et al., 1998). However, this was not the case for HB-EGF. We have performed ex vivo transfection of $HB^{\Delta tm}$ cDNA into mouse embryonic skin (Fig. S3 and supplemental Results, available at http://www.jcb.org/cgi/content/full/jcb.200307035/DC1). Transfection of $HB^{\Delta tm}$, but not WT proHB-EGF, resulted in embryonic epidermal hyperplasia. CRM197, a protein that specifically inhibits the mitogenic activity of HB-EGF (Mitamura et al., 1995), inhibited HB-ΔTM–induced hyperplasia. As CRM197 is membrane impermeable, hyperplasia induced by transfection with $HB^{\Delta tm}$ must be mediated by secreted HB-ΔTM in a paracrine manner.

In conclusion, proHB-EGF shedding and the strict control of this process are essential for the function of this growth factor. Not only HB-EGF, but also other EGF family growth factors and cytokines are synthesized as membrane-anchored forms. The present study suggests that the strict control of ectodomain shedding is essential for the physiological function of these membrane-anchored ligands. This study also indicates that posttranslational regulation, in addition to transcriptional control, is crucial for the function of membrane-anchored growth factors.

Materials and methods

Northern blotting

Total RNA was isolated from tissues using ISOGEN (Nippon Gene), according to the manufacturer's instructions. Details of the hybridization procedure are shown in the supplemental Materials and methods (available at http://www.jcb.org/cgi/content/full/jcb.200307035/DC1).

Immunoblotting of tissues

For the detection of HB-EGF and HB-UC in adult skin, back skin from 11-wk-old $HB^{lox/lox}$ and $HB^{uc/uc}$ mice was treated with 800 nmol of tRA for 3 d. 2 h before specimen isolation, the back skin was additionally treated with 8 nmol of TPA. The isolated full back skin was homogenized in lysis buffer (Iwamoto et al., 2003). For detection of HB-ΔTM in neonatal skin, skin from P1 $HB^{\Delta tm}$ heterozygous mice or WT littermates was homogenized in lysis buffer. Details of the immunoblotting procedure using these lysate samples are shown in the supplemental Materials and methods (available at http://www.jcb.org/cgi/content/full/jcb.200307035/DC1).

Histological analysis

Mouse hearts were fixed by perfusion with 4% paraformaldehyde, dehydrated, and embedded in paraffin. 4-μm sections were stained with either hematoxylin-eosin or Azan-Mallory. For immunohistochemical analysis of transplanted skin, specimens of full-thickness skin (2–3 cm^2) were transplanted onto the backs of Balb/c nu/nu mice (8 wk old) and then fixed with adhesive bandages for 1 wk. 2 wk after transplantation, skin specimens were isolated from the grafted skin and subjected to immunohistochemical analysis. Information of the used antibodies for immunohistochemistry, microscopy, and image processing is shown in the supplemental Materials and methods (available at http://www.jcb.org/cgi/content/full/jcb.200307035/DC1).

Echocardiography

Transthoracic echocardiograph was performed with a cardiac ultrasound recorder (SONOS 5500; Hewlett-Packard) with a 15-MHz transducer, as described previously (Iwamoto et al., 2003).

RT-PCR

RNA was isolated from tissues of P14 mice using TRIzol reagent (Invitrogen). Reverse transcription was performed using a reverse transcriptase, ReverTra Dash (TOYOBO). Primer sets used in PCR analyses are shown in the supplemental Materials and methods (available at http://www.jcb.org/cgi/content/full/jcb.200307035/DC1).

Online supplemental material

The supplemental material is available at http://www.jcb.org/cgi/content/full/jcb.200307035/DC1. Fig. S1 shows the characterizations of HB-UC and HB-ΔTM. Fig. S2 shows the targeting construct of HB^{uc} and $HB^{\Delta tm}$ and genotypic analyses. Fig. S3 shows ex vivo transfection of $HB^{\Delta tm}$ cDNA into mouse embryonic skin. Supplemental Results, Materials and methods, and References are also presented.

We thank I. Ishimatsu, M. Hamaoka, and T. Yoneda for technical assistance.

This work was supported by the Research for the Future Program of the Japan Society for the Promotion of Science (97L00303 for E. Mekada) and by Grants-in-Aid from the Ministry of Education, Culture, Sports, Science, and Technology (12215152 and 14032202 for E. Mekada and 12680705 for R. Iwamoto).

Submitted: 7 July 2003
Accepted: 12 September 2003

References

Chen, B., R.T. Bronson, L.D. Klaman, T.G. Hampton, J.F. Wang, P.J. Green, T. Magnuson, P.S. Douglas, J.P. Morgan, and B.G. Neel. 2000. Mice mutant for Egfr and Shp2 have defective cardiac semilunar valvulogenesis. *Nat. Genet.* 24:296–299.

Crone, S.A., Y.Y. Zhao, L. Fan, Y. Gu, S. Minamisawa, Y. Liu, K.L. Peterson, J. Chen, R. Kahn, G. Condorelli, et al. 2002. ErbB2 is essential in the prevention of dilated cardiomyopathy. *Nat. Med.* 8:459–465.

Elenius, K., S. Paul, G. Allison, J. Sun, and M. Klagsbrun. 1997. Activation of HER4 by heparin-binding EGF-like growth factor stimulates chemotaxis but not proliferation. *EMBO J.* 16:1268–1278.

Goishi, K., S. Higashiyama, M. Klagsbrun, N. Nakano, T. Umata, M. Ishikawa, E. Mekada, and N. Taniguchi. 1995. Phorbol ester induces the rapid processing of cell surface heparin-binding EGF-like growth factor: conversion from juxtacrine to paracrine growth factor activity. *Mol. Biol. Cell.* 6:967–980.

Heid, H.W., I. Moll, and W.W. Franke. 1988. Patterns of expression of trichocytic and epithelial cytokeratins in mammalian tissues. II. Concomitant and mutually exclusive synthesis of trichocytic and epithelial cytokeratins in diverse human and bovine tissues (hair follicle, nail bed and matrix, lingual papilla, thymic reticulum). *Differentiation.* 37:215–230.

Higashiyama, S., J.A. Abraham, J. Miller, J.C. Fiddes, and M. Klagsbrun. 1991. A heparin-binding growth factor secreted by macrophage-like cells that is related to EGF. *Science.* 251:936–939.

Higashiyama, S., K. Lau, G.E. Besner, J.A. Abraham, and M. Klagsbrun. 1992. Structure of heparin-binding EGF-like growth factor. Multiple forms, primary structure, and glycosylation of the mature protein. *J. Biol. Chem.* 267:6205–6212.

Hirata, M., T. Umata, T. Takahashi, M. Ohnuma, Y. Miura, R. Iwamoto, and E. Mekada. 2001. Identification of serum factor inducing ectodomain shedding of proHB-EGF and studies of noncleavable mutants of proHB-EGF. *Biochem. Biophys. Res. Commun.* 283:915–922.

Iwamoto, R., and E. Mekada. 2000. Heparin-binding EGF-like growth factor: a juxtacrine growth factor. *Cytokine Growth Factor Rev.* 11:335–344.

Iwamoto, R., S. Yamazaki, M. Asakura, S. Takashima, H. Hasuwa, K. Miyado, S. Adachi, M. Kitakaze, K. Hashimoto, G. Raab, et al. 2003. Heparin-binding EGF-like growth factor and ErbB signaling is essential for heart function. *Proc. Natl. Acad. Sci. USA.* 100:3221–3226.

Izumi, Y., M. Hirata, H. Hasuwa, R. Iwamoto, T. Umata, K. Miyado, Y. Tamai, T. Kurisaki, A. Sehara-Fujisawa, S. Ohno, and E. Mekada. 1998. A metalloprotease-disintegrin, MDC9/meltrin-γ/ADAM9 and PKCδ are involved in TPA-induced ectodomain shedding of membrane-anchored heparin-binding EGF-like growth factor. *EMBO J.* 17:7260–7272.

Jackson, L.F., T.H. Qiu, S.W. Sunnarborg, A. Chang, C. Zhang, C. Patterson, and D.C. Lee. 2003. Defective valvulogenesis in HB-EGF and TACE-null mice is associated with aberrant BMP signaling. *EMBO J.* 22:2704–2716.

Massague, J., and A. Pandiella. 1993. Membrane-anchored growth factors. *Annu. Rev. Biochem.* 62:515–541.

Mitamura, T., S. Higashiyama, N. Taniguchi, M. Klagsbrun, and E. Mekada. 1995. Diphtheria toxin binds to the epidermal growth factor (EGF)-like domain of human heparin-binding EGF-like growth factor/diphtheria toxin receptor and inhibits specifically its mitogenic activity. *J. Biol. Chem.* 270:1015–1019.

Ozcelik, C., B. Erdmann, B. Pilz, N. Wettschureck, S. Britsch, N. Hubner, K.R. Chien, C. Birchmeier, and A.N. Garratt. 2002. Conditional mutation of the ErbB2 (HER2) receptor in cardiomyocytes leads to dilated cardiomyopathy. *Proc. Natl. Acad. Sci. USA.* 99:8880–8885.

Takenobu, H., A. Yamazaki, M. Hirata, T. Umata, and E. Mekada. 2003. The stress- and inflammatory cytokine-induced ectodomain shedding of heparin-binding epidermal growth factor-like growth factor is mediated by p38 MAPK, distinct from the 12-O-tetradecanoylphorbol-13-acetate- and lysophosphatidic acid-induced signaling cascades. *J. Biol. Chem.* 278:17255–17262.

Umata, T., M. Hirata, T. Takahashi, F. Ryu, S. Shida, Y. Takahashi, M. Tsuneoka, Y. Miura, M. Masuda, Y. Horiguchi, and E. Mekada. 2001. A dual signaling cascade that regulates the ectodomain shedding of heparin-binding epidermal growth factor-like growth factor. *J. Biol. Chem.* 276:30475–30482.

Werner, S., W. Weinberg, X. Liao, K.G. Peters, M. Blessing, S.H. Yuspa, R.L. Weiner, and L.T. Williams. 1993. Targeted expression of a dominant-negative FGF receptor mutant in the epidermis of transgenic mice reveals a role of FGF in keratinocyte organization and differentiation. *EMBO J.* 12:2635–2643.

Wiley, H.S., M.F. Woolf, L.K. Opresko, P.M. Burke, B. Will, J.R. Morgan, and D.A. Lauffenburger. 1998. Removal of the membrane-anchoring domain of epidermal growth factor leads to intracrine signaling and disruption of mammary epithelial cell organization. *J. Cell Biol.* 143:1317–1328.

Xiao, J.H., X. Feng, W. Di, Z.H. Peng, L.A. Li, P. Chambon, and J.J. Voorhees. 1999. Identification of heparin-binding EGF-like growth factor as a target in intercellular regulation of epidermal basal cell growth by suprabasal retinoic acid receptors. *EMBO J.* 18:1539–1548.

The Journal of Cell Biology